Journal of the European Ceramic Society 19 (1999) 7–15

PII: S0955-2219(98)00161-7
0955-2219/98/$—see front matter

Stability of α-Sialons in Low Temperature Annealing

Mamoru Mitomo* and Akira Ishida†

National Institute for Research in Inorganic Materials, 1-1, Namiki, Tsukuba-shi, Ibaraki, 305, Japan

(Received 6 April 1998; accepted 16 June 1998)

Abstract

Phase and microstructural change due to post-sintering annealing of Nd, Dy, Y and Yb-α-sialon ceramics have been investigated for the composition of α-sialon-rare earth aluminum garnet (RAG) systems. For R= Dy, Y and Yb, only α-sialon was observed as the crystalline phase after sintering at 1750°C. After subsequent post-sintering annealing at 1450°C for 72 h, no phase transformation from α-to β-sialon was observed, although the crystallization of garnet phase at grain boundaries was detected. However, for R=Nd, α-,β-sialon and melilite phase (M') were observed after sintering at 1750°C. The β-sialon and melilite phases increased with low-temperature heat treatment, implying that the transformation from α- to β-sialon occurred. It was concluded that the α-sialon phase stabilized by small ions like Y, Dy or Yb has high thermal stability and does not transform to β-sialon when there is no chemical reaction between α-sialon grains and the grain boundary phase. © *1998 Elsevier Science Limited. All rights reserved*

Keywords: sialon, microstructure-final, annealing, grain boundaries, Si_3N_4

1 Introduction

Silicon nitride based ceramics are fabricated by liquid phase sintering. The mechanical properties are directly related to the microstructures of ceramics.[1] Because of the detrimental effect of the grain boundary glassy phase, the elimination of liquid phase by dissolving into grains which results in the formation of sialons, has been investigated.[1,2] The α-sialon ceramics are particularly interesting due to their wide varieties of chemical compositions, microstructures and resulting mechanical properties.[3–5] The α-structure is stabilized by metal dissolution into interstitial sites and concurrent substitution of Al and O into Si and N site, respectively. There is not only maximum but also minimum values for the stabilization of α-structure, i.e. $x \fallingdotseq 0{\cdot}3$ in the general formula Rx(Si, Al)$_{12}$ (O,N)$_{16}$.[6,7] In the region $O < x < 0{\cdot}3$, the composite microstructures consisted of fine equiaxial α-grains, and elongated β-Si_3N_4 grains develop.[3] The hardness and strength of sintered ceramics depend on the α/β ratio. High strength and fracture toughness result from reinforcement by elongated β-Si_3N_4 grains. This type of material provides a typical example of *in situ* reinforcement.

Although there have been many works on the relation between chemical compositions, phase compositions and microstructures,[3–9] it was quite recently that the phase transformation of α-sialon to β-sialon during low temperature annealing was reported.[10–16] The microstructures of sintered materials are directly related to the α/β ratio.[11,17,18] Therefore, it is necessary to understand the mechanism of phase transformation to tailor the microstructures of sialons.

Experimental results on the stability of α-sialons in post-sintering heat treatment shown below are reported.

1. The phase change should accompany the change in chemical composition in grains together with structural change.[14,15,19] If the α-or β-sialon is represented by α' or β' for simplicity,

$$\alpha'_1 + (\beta'_1) + G_1 \rightarrow (\alpha'_2) + \beta'_2 + G_2(orC) \qquad (1)$$

where G and C represent the glassy and crystalline phase, respectively. Therefore, the stability of α-sialon largely depends on the amount and the chemical composition of the grain boundary glassy phase.

2. It is likely that the nucleation of a new phase is the rate determining step because the rate of

*To whom correspondence should be addresed.
†Present address: Isuzu Ceramics Research Institute Co., Ltd. 8 Tsuchidana, Fujisawa-shi, Kanagawa-ken, 252, Japan.

$\alpha' \rightarrow \beta'$ phase transformation is directly related to the amount of β' in as-sintered materials.[13,15]

3. The apparent stability of α-sialon is also related to the ionic radius of stabilizing metals.[17] However, the α'/β' ratio in sintered materials depends largely on kinetics of α-sialon formation, i.e. small ions dissolve more easily into an α-lattice. Large metals tend to produce larger amounts of β-sialon and residual glassy phase under the same chemical composition and processing conditions.[15,20]

It is therefore difficult to determine the stability relation of α- and β-sialon from published experimental results with varying amounts of glassy phase or β-sialon because the presence of glassy phase accelerates the grain boundary diffusion, whereas it works as a reactant as shown in eqn (1). However, if the materials fabricated from the stoichiometric compositions for α-sialons were annealed at low temperature, there was no appreciable change simply because of the slow rate of grain boundary diffusion. Therefore, it is necessary to examine the stability of α-sialons at low temperatures in the presence of inert glassy phase.

Y-α-sialon is in equilibrium with a liquid of yttrium aluminum garnet (YAG) composition at 1750°C. The garnet crystallized during annealing at 1450°C.[21] There is no chemical reaction between α-sialon grains and grain boundary phase in this system. The difference in free energy between reactants and products for post-sintering heat treatment is similar to that between amorphous and crystalline YAG phase at grain boundaries. The stability of α-sialon during post-sintering heat treatment might therefore be directly compared. Moreover, there is enough glassy phase in this system to provide enough diffusion if phase change is to occur.

2 Experimental Procedure

The α-sialon can be formed according to the following equation,

$$(4 - 1.5x)Si_3N_4 + 0.5x(R_2O_3 + 9AlN) \rightarrow R_x(Si_{12-4.5x}Al_{4.5x})(O_{1.5x}N_{16-1.5x}) \quad (2)$$

where M is a lanthanide metal or Y. In the present work, R = Nd, Dy, Y or Yb was used with the composition of $x = 0.45$. Rare earth aluminum garnet composition ($R_3Al_5O_{12}$, RAG) 10 wt% was also added to the R-α-sialon composition.

Si_3N_4 (Ube Industries Co., Tokyo, Japan, SN-E10), AlN (Tokuyama, Tokyo, Japan, Type F), Nd_2O_3, Dy_2O_3, Y_2O_3, Yb_2O_3 (Shin-etsu Chemical Co., Tokyo, Japan, 99.9% pure) and Al_2O_3 (Sumitomo Chemicals Co., Osaka, Japan, AKP-20) powders were used as the starting materials. About 15 g of powder mixture was mixed in hexane using a Si_3N_4 pot and Si_3N_4 balls for 2 h in a planetary mill. About 3 g of dried powder was hot-pressed at 1750°C for 1 h using a graphite die lined with BN under a pressure of 20 MPa in static nitrogen of 0·1 MPa. The temperature was raised at a rate of 30°C min^{-1}. Cooling rate was about 100°C min^{-1} from 1750 to 1350°C. The densification behavior during heating was monitored by a dilatometer.

Hot-pressed specimens were heat treated at 1450°C for 72 h in nitrogen atmosphere to examine the stability of α-sialons at low temperature. After the heat treatment, Y- and Nd-containing samples were heated again to 1750°C to investigate the phase and microstructure change. Dy- and Yb-containing samples behave similarly to the Y-containing one and are not examined here. Nd has the largest ionic size among Nd, Dy, Y and Yb and exhibits different stabilizing and annealing behavior.[18–22]

Crystalline phases were determined by X-ray diffraction analysis (XRD). The amounts of α- and β-sialon phases were determined using the intensifies of the (102) reflection of α-sialon and the (101) reflection of β-sialon.[11] Unit cell dimensions were determined by XRD using Si as an internal standard. The solid solubility in α-sialon is shown by x in the general formula, $M_x\ Si_{12-(m+n)}\ Al_{m+n}\ O_nN_nN_{16-n}$. Shen and co workers reported that the a and c values in hexagonal cell of α-sialon are related to the solid solubility as shown below irrespective of the ionic size of the stabilizing metal.[18,22]

$$a(nm) = 0.775 + 0.0156X_a \quad (3)$$

$$c(nm) = 0.562 + 0.0162X_c \quad (4)$$

The average value of X_a and X_c was used as the solid solubility (x) in the present work.

Solid solubility (z) in β-sialon ($Si_{6-z}Al_zO_zN_{8-z}$) was also calculated from the cell dimensions using known relations.[23] The change in chemical composition due to post-sintering annealing was detected by determining the cell sizes of sialons.

Sintered and heat-treated samples were cut and polished then observed by a scanning electron microscope (SEM). Back scattering electrons were collected to identify α-sialon, β-sialon and glassy phase by their contrast.[15] The metallic composition in crystalline grains was determined by EDS analysis. The composition of β-sialon and melilite phase (M') with the formula $R_2\ Si_{3-x}\ Al_x\ O_{3+x}\ N_{4-x}$[14,24] in the Nd-system was determined

qualitatively. The quantitative evaluation was difficult because of the incorporation of signals from grain boundary phase due to small grain size.

3 Results and Discussion

3.1 Densification behavior

The densification curves during hot-pressing to 1750°C are shown in Figure 1. Densification occurs in two steps. The low temperature sintering at 1400 to 1500°C is supposed to be due to the rearrangement process. The nitride particles are wetted by the oxide melt at this stage.[25] The densification at higher temperature is supposed to be due to the dissolution of nitrides or intermediate oxynitride phases and the precipiitation as α-sialon.[25–27] Figure 1 shows that the densification curves are classified into two groups depending on the difference in high temperature densification behavior. One (Y and Yb) densities at high temperature and in a narrow temperature range. The other (Nd and Dy) densities over a wider temperature range (1550–1700°C). The wider range might be related to a smaller amount of transient liquid based on the oxynitride formation in an intermediate stage. An oxynitride of melilite structure (M') remained in the Nd-system even after sintering at 1750°C for 1 h. High relative density >98% was in all systems obtained when the temperature reached 1750°C. The difference in final density in Fig. 1 is due to that of α-sialon and RAG phase containing different lanthanide metal.

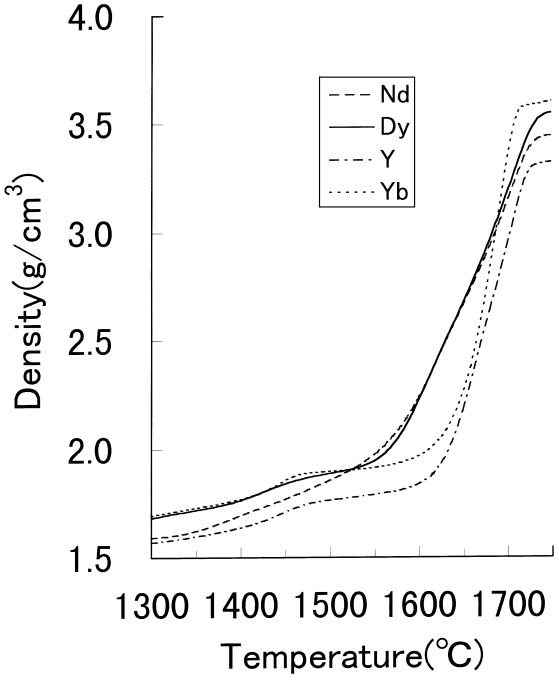

Fig. 1. Densification curve during heating at a rate of 30°C min^{-1} up to 1750°C.

3.2 Phase change during low temperature annealing

Table 1 presents crystalline phases in as-sintered and heat-treated samples. After sintering at 1750°C for 1 h, only α-sialon was observed for M = Y, Dy and Yb. However, when M = Nd was used, α-sialon, β-sialon and melilite were observed. After the Y, Dy and Yb-containing samples were annealed at 1450°C for 72 h, α-sialon and garnet (RAG) were observed. This shows that garnet crystallizes from the glassy phase during heat treatment. The α contents in as-sintered and annealed specimens are shown in Figs 2 and 3, respectively. The smaller amount of α-sialon in the Nd-system compared to other systems is due both to the β-sialon and melilite(M') formation. The selective formation of melilite phase by the reaction between Si_3N_4 and rare earth oxide during the preparation of α-sialon was observed when the ionic radius was large like Nd, Sm or Dy.[18,24,28] It was also shown that these α-sialons decomposed by reactions shown below during low temperature annealing[22,24]

$$\alpha_1 + G \rightarrow \alpha_2 + M' \tag{5}$$

$$\alpha + G \rightarrow \beta + M' \tag{6}$$

The decrease of α-content in the Nd-system in Fig. 3 is due to the increase in β and M' content in accordance with eqn (6). Clearly Y-, Dy- and Yb-α-sialon did not transform to β-sialon when the α sialon garnet system was used even if there is enough grain boundary phase for the diffusion.

It has been reported that the α to β transformation rate in (α + β) composites depends largely on the amount of grain boundary glassy phase and the type of stabilizing metal. Previous data[11,15] are also

Table 1. Crystalline phases in as-sintered and annealed specimens

	Sample name	*XRD*			
		α	β	*RAG*	M′
Nd system					
Sintered at 1750°C	NdS	s	m	—	m
Annealed at 1450°C	NdA	—	s	—	m
Re-heated at 1750°C	NdH	—	s	—	m
Dy system					
Sintered at 1750°C	DyS	s	—	—	—
Annealed at 1450°C	DyA	s	—	m	—
Y system					
Sintered at 1750°C	YS	s	—	—	—
Annealed at 1450°C	YA	s	—	m	—
Re-heated at 1750°C	YH	s	w	—	—
Yb system					
Sintered at 1750°C	YbS	s	—	—	—
Annealed at 1450°C	YbA	s	—	m	—

RAG: rare earth aluminum garnet.
M′: melilite phase.
s, Strong; m, medium; w, weak.

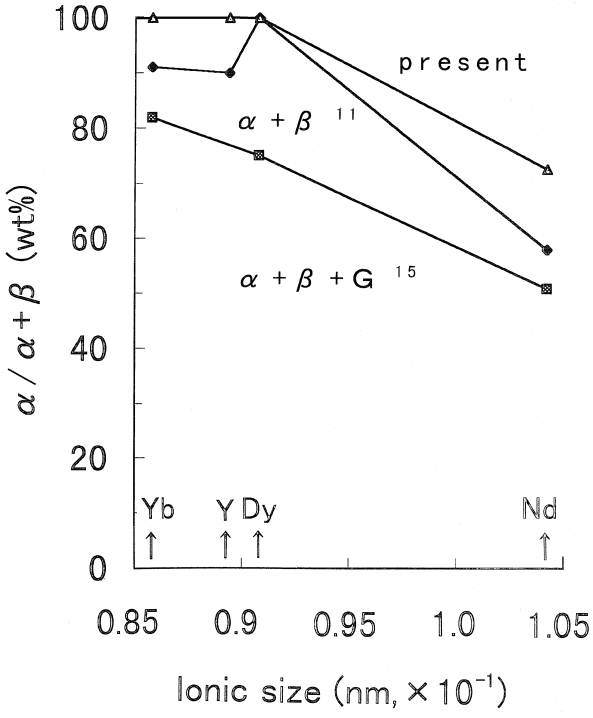

Fig. 2. α Content in as-sintered specimens as a function of ionic size of rare earth metals. Reported relations[11,15] are also plotted for comparsion.

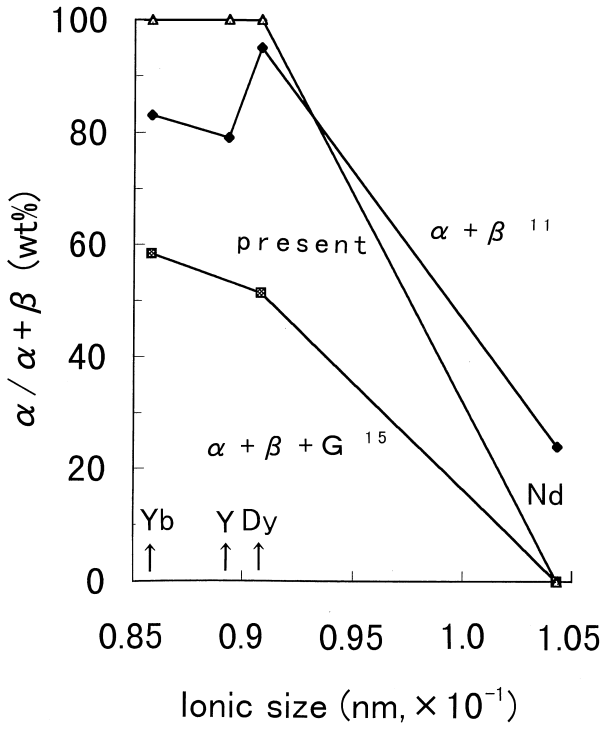

Fig. 3. α Content in annealed specimens at 1450°C for 72 h compared with other data.[11,15]

shown in Figs 2 and 3 for comparison. The $(\alpha+\beta)$ composites prepared from α single-phase α-sialon composition (shown as $\alpha+\beta$ in the figures) have some β phase, the content of which depends on the type of stabilizing metal.[11] There is less α phase in sintered Nd-α-material than in other metals because of the formation of melilite (M') phase which agreed with the result of present work. The α content decreased after annealing at 1450°C for 72 h. It is interesting to note that even single-phase Dy-α-sialon transformed partly to β-sialon during annealing. This suggests that the nucleation of new phase (β-sialon) should not be the rate determining step in the phase transformation. It is likely that the transformation is due to the chemical reaction between α-sialon and oxide rich glass as shown in eqn (1). The other composition, which has more β and glassy phase (shown as $\alpha+\beta+G$ in the figures), was also studied to examine the stability in low temperature annealing.[15] The nominal composition was for the formation of 70% $\alpha-$ and 30% β-sialon. They transform more easily than those of $(\alpha+\beta)$ composites. The grain boundary glassy phase is thus suggested to accelerate grain boundary diffusion and to form β-sialon through the reaction with α grains. In fact, when the $(\alpha+\beta)$ composites were prepared from stoichiometric composition in Y- and Yb-systems, there was no appreciable change in the α/β ratio, even after annealing for 30 days at 1450°C.[17] This means that the phase transformation from α- to β-sialon should be regarded as the result of the chemical reaction revealed by eqn (1).

In the present work, the glassy phase of the RAG composition should provide enough path for grain boundary diffusion. The increase in β content in the Nd-system is based on the similar chemical reaction as in previous works.[11,15] The absence of phase transformation in the Dy, Y and Yb-systems is based on the higher thermodynamic stability than the Nd-system, which might be related to the higher stabilization effect[11] and wider solid solubility[6] in the system containing small stabilizing metals. Although the glassy phase with RAG composition existed with α-sialon grain in the present work, there was no substantial reaction between them because of the stability of the two phases.[21] We concluded that α-sialons containing small metals like Dy, Y or Yb, do not transform to β-sialon in the absence of oxide reactants.

3.3 Microstructural change during annealing

The microstructures of as-sintered materials are shown in Fig. 4. The micrographs of a Dy-, Y- and Yb-systems [Fig. 4(b)–(d)] have a similar microstructure. The α-sialon grains (gray) are surrounded by glassy phase (white). In contrast, the Nd-system has a quite different microstructure. In addition to α-sialon grains and glassy phase, β-sialon grains (black) and M' phase (large white) were also detected.

After annealing at 1450°C, the microstructures change very much in the morphology of grain boundary phase as shown in Fig. 5. XRD shows that the glassy phase crystallized as rare earth

aluminum garnet (RAG). The materials consisted of two phases, β-sialon + M′ in the Nd-system and α-sialon + RAG in other systems. The coalescence of the oxide phase is clearly shown together with the higher dihedral angle between RAG and sialon grains. Higher strength of heat-treated materials than as-sintered ones at high temperature is shown in accord with their microstructures.[28]

Similar behavior in the morphology change during annealing was reported in α + β-sialon systems.[29] As the chemical composition of β-sialon is closer to that of the grain boundary phase than to that of α-sialon, β-sialon can adsorb excess oxide over YAG phase at the grain boundary. This might be why sialon grains dewetted from YAG phase in α + β sialon during annealing. In the present work, α-sialon and glassy phase did not react because the reaction should always result in the formation of β-sialon. It means that only crystallization of the RAG phase occurred during annealing in the Dy-,Y- and Yb-systems.

3.4 Composition change

Unit cell dimensions of α-sialon and β-sialon in as-sintered and annealed materials are listed in Table 2, together with calculated x values in α-sialon and z values in β-sialon. The x values are lower than that calculated from the starting composition, i.e. $x = 0{\cdot}45$. This indicates that a small amount of rare earth oxide and AlN remained in grain boundaries. It is interesting to note that the x value after low temperature annealing depends largely on the size of this stabilizing ion. The x value in the Yb-system increased from 0·33 to 0·37, whereas that in Dy- and Y-system decreased from 0·38 to 0·30 and 0·39 to 0·36, respectively.

It has been reported that cell dimensions of α-sialon in α + β composites decreased a little at a very early stage of annealing in Y- and Yb-systems.[17] They did not show any appreciable change with further annealing. This evidence supports the idea that α-sialon of the Y-, Dy- or Yb-system is stable at low temperature when there was no reactive oxide at grain boundaries. In contrast, a slow decrease of α-content in the Sm-system[12] and sharp decrease in the Nd-system[17] during annealing was reported. The results of the present investigation agreed well with those of previous investigations[15,17,22] in that the decrease of α-content is followed by the increase in β-and M'-content.

3.5 Re-heating at 1750°C

Several reports have been published recently on α→β transformation during low-temperature heat treatment.[10,13,15,18] They investigated the effect of starting composition, the type of stabilizing metal, and the amount and the composition of glassy phase on the stability of α-sialon at low temperatures

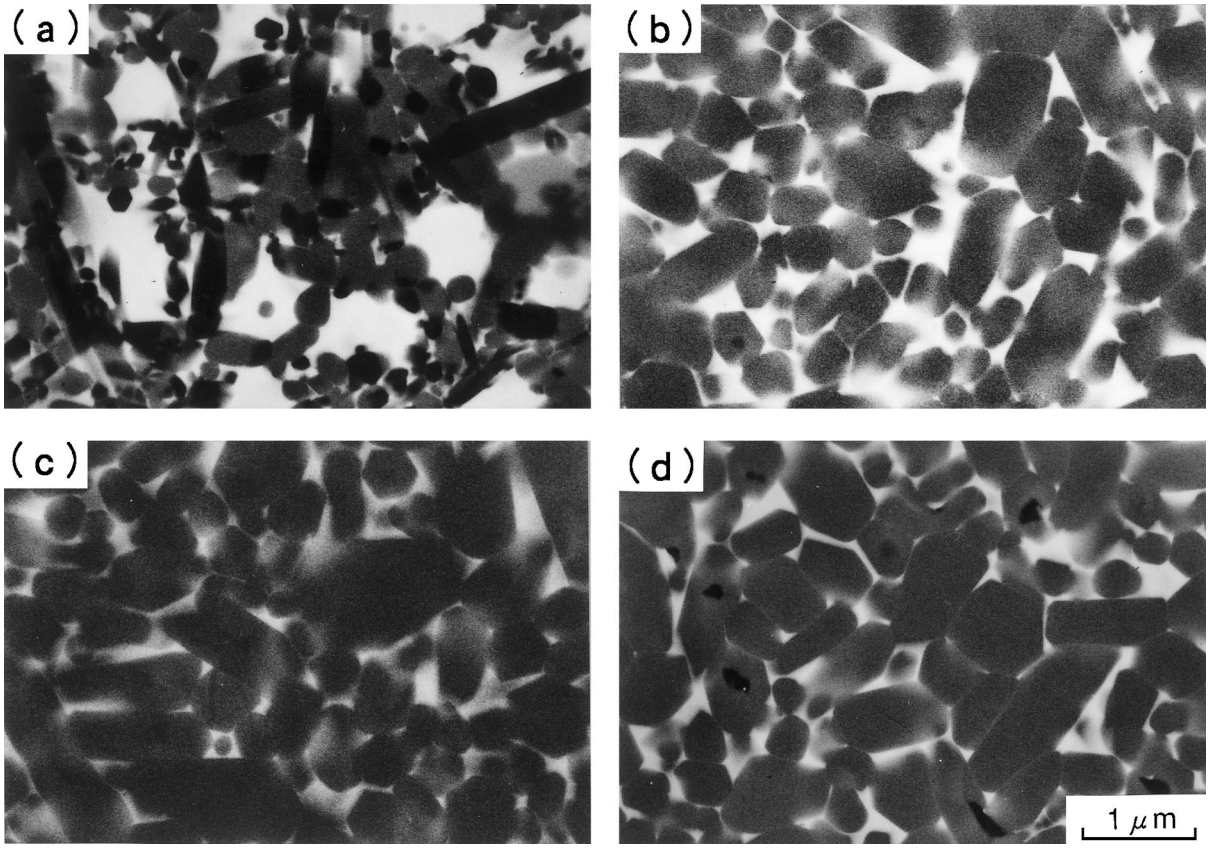

Fig. 4. SEM micrograph of as-sintered specimens from (a) Nd-, (b) Dy-, (c) Y-, and (d) Yb-systems.

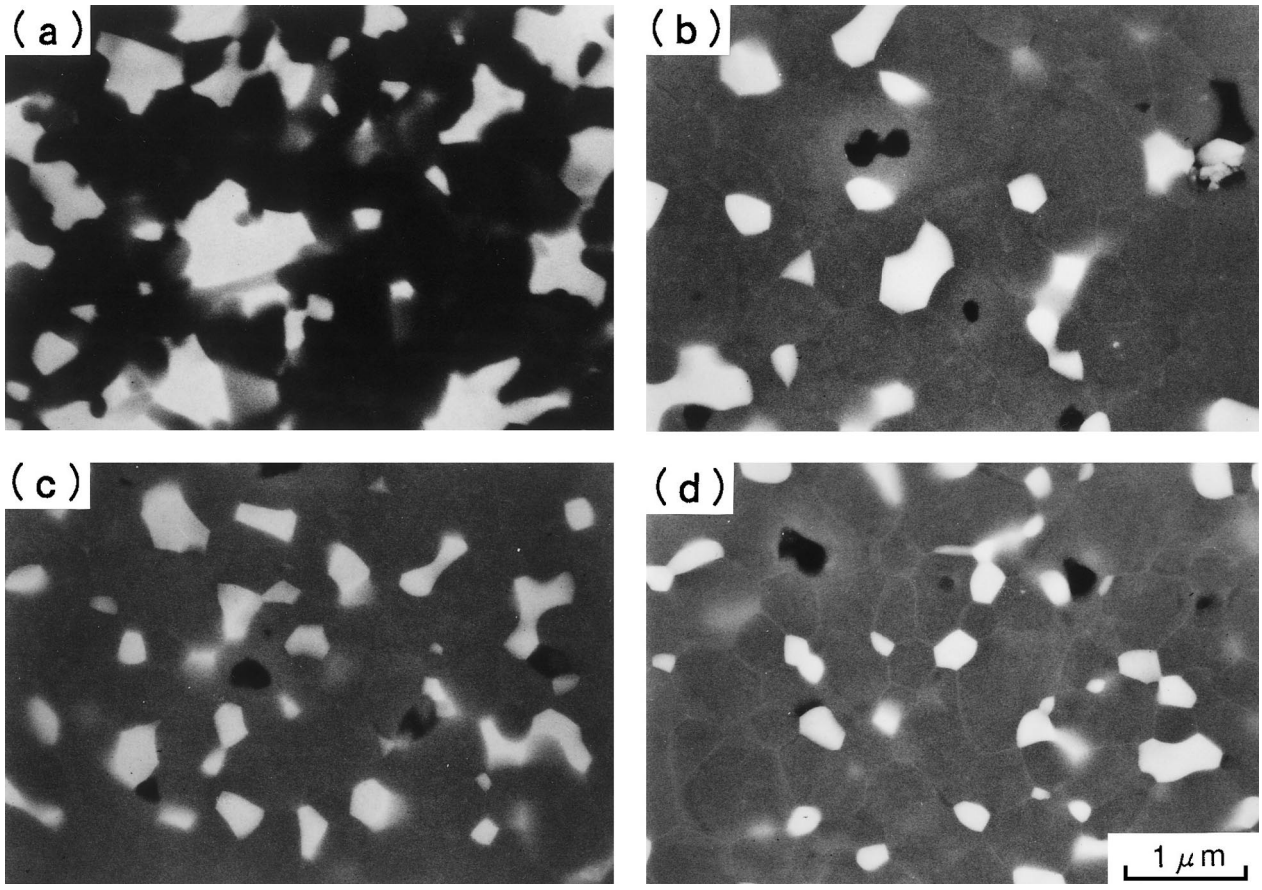

Fig. 5. SEM micrograph of specimens of (a) Nd-, (b) Dy-, (c) Y-, and (d) Yb-systems after annealing at 1450°C.

Table 2. Unit cell dimensions and calculated solubilities of α- and β-sialon in as-sintered and annealed specimens

Sample	*Unit cell of* (*nm*)		*Calculated solubility* (x)	*Unit cell of* β (*nm*)		*Calculated solubility* (z)
	a	c		a	c	
Nd System						
NdS	0·7795	0·5681	0·33	0·7618	0·2915	0·41
NdA				0·7612	0·2917	0·35
NdH				0·7603	0·2914	0·14
Dy System						
DyS	0·7801	0·5689	0·38	—	—	—
DyA	0·7797	0·5668	0·30	—	—	—
Y system						
YS	0·7807	0·5686	0·39	—	—	—
YA	0·7801	0·5684	0·36	—	—	—
YH	0·7805	0·5687	0·38	—	—	—
Yb system						
YbS	0·7798	0·5678	0·33	—	—	—
YbA	0·7799	0·5688	0·37	—	—	—

(< 1550°C). Some of them refer to a $\alpha \Longleftrightarrow \beta$ phase transformation that can be reversed by changing the temperature. However, it seems that only one paper has really reported the $\beta \rightarrow \alpha$ reverse transformation by re-heating at higher temperature.[27]

The present work has shown that the microstructural change occurred by low temperature annealing Y-, Dy- or Yb- α-sialon even though there was no phase transformation. It is quite interesting to investigate the microstructure after re-heating at high temperature. The microstructures of Nd- and Y- a -sialon after reheating at 1750°C for 1 h are shown in Fig. 6. The microstructure of Y-α-sialon was basically similar to that of the as-sintered material [Fig. 4(c)], although a little grain growth of α-sialon was observed. The α-sialon grains were wetted well again by the penetration of glassy phase into grain boundaries. Cell dimensions were also increased as shown in Table 2. This means that the microstructure of Y-α-sialon

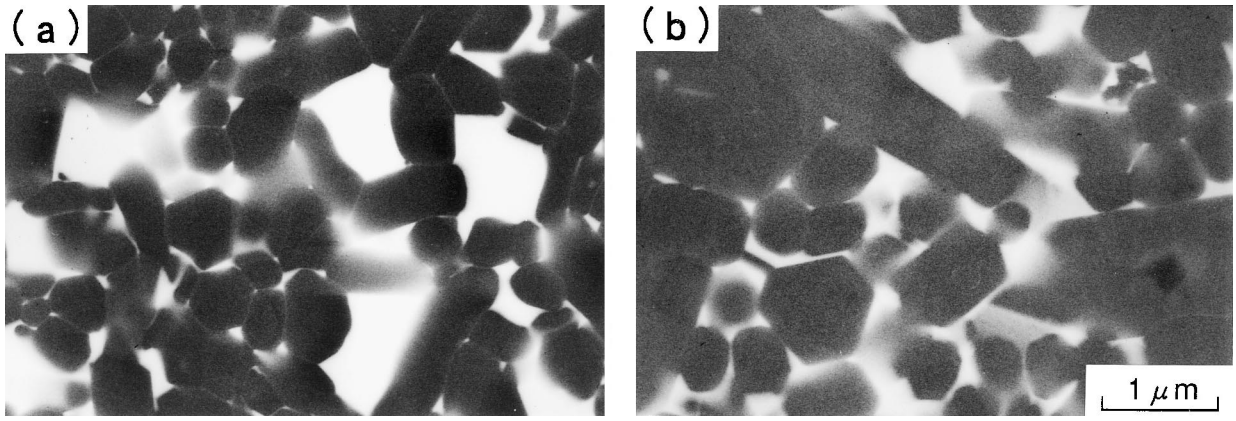

Fig. 6. SEM micrograph of specimens of (a) Nd, (b) Y-systems after re-heating at 1750°C.

recovered completely by re-heating at high temperature. The main change depending on temperature change was thus revealed to be the decrease of solid solubility and the crystallization of YAG phase at low temperature. In the Nd-system, the penetration of glassy phase was also observed. However, the transformation of β to α grains was not observed. Thus, partial recovery of microstructure took place in the Nd-system. The changes in XRD after annealing and subsequent re-heating of the Nd- and Y systems together with as-sintered material are shown in Figs 7 and 8, respectively. There was no β-to-α phase transformation during re-heating at 1750°C in the present work.

Mandal and Thompson[27] observed the reversible $\alpha \Longleftrightarrow \beta$ change in XRD and microstructure of Dy-system. The α content in the as-sintered material decreased from 63 to 8% after annealing for 60 h at 1450°C. Re-heating at 1800°C for 15 min restored the microstructure as in the as-sintered material. Although they explained the ease of transformation from α to β at low temperature based on the amount and composition of glassy phase, they showed no reason for the reversible $\beta \rightarrow \alpha$ change.

The results of EDS analysis of the re-heated specimen in the Nd-system are shown in Fig. 9. Qualitative evaluation revealed that black grains [Fig. 9 (a)] consist of Si and Al metallic constituents, implying that they are β-sialon grains. The analysis also indicates that white grains [Fig. 9(b)] consist of Nd, Si and Al, i. e. melilite phase. Therefore, large white grains in Figs 3(a) and 4(a) were also determined to be melilite grains.

3.6 Effect of temperature on the stability of α-sialon

The present work showed that the solubility of stabilizing metal in α-sialon depends on temperature. The solubility is generally higher at high temperature and lower at low temperature. Instability of Nd-α-sialon in the presence of β and glassy phase at low temperature was also shown.

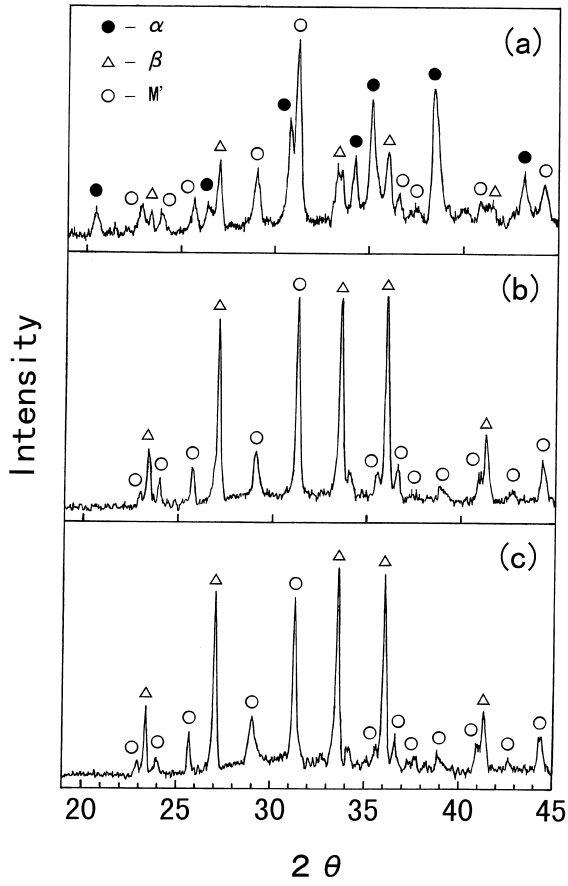

Fig. 7. XRD profile of Nd-system, (a) as-sintered, (b) annealed at 1450°C, and (c) re-heated at 1750°C.

The stabilities of Dy, Y- and Yb- α-sialons are explained by the fact that the composition remained in the stability range. We have shown that the α-sialon stabilized by a large ion shifts more to lower x values than that stabilized by a smaller ion. Most likely, the composition in Nd-α-sialon shifted to a value below the critical values and resulted in the $\alpha \rightarrow \beta$ transformation.

It seems likely that the relative stability of α-sialon in the Nd-system may be low because of the larger stress caused by the incorporation of

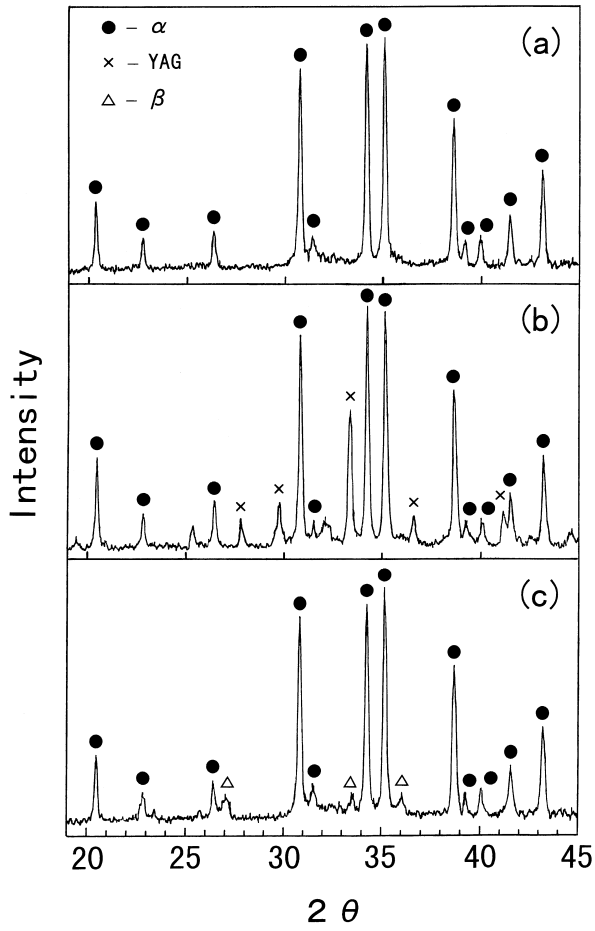

Fig. 8. XRD profile of Y-system, (a) as-sintered, (b) annealed at 1450°C, and (c) re-heated at 1750°C.

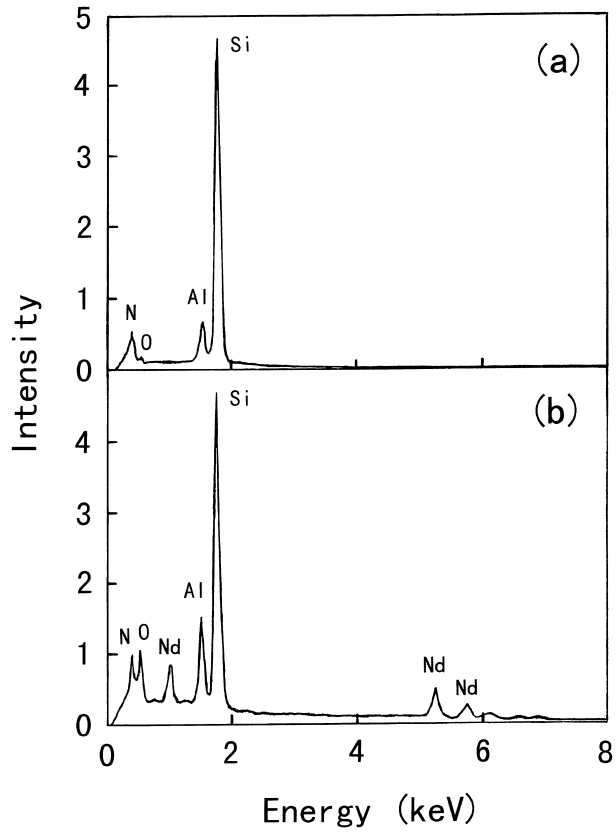

Fig. 9. EDS spectrum from annealed specimen in Nd-system, (a) β-sialon, and (b) melilite (M′) phase.

large metal at interstitial site as compared to incorporation into the melilite phase. The M' phase formation competes with α-sialon formation in consuming rare earth oxide. It has been shown that the minimum value for the stabilization is about $x = 0{\cdot}3$, irrespective of ionic size.[6,7] However, their data are based on equilibrium experiments. It is well known that α-structure stability decreases with large rare earth metals because the α-content decreases with ionic radius of rare earth metals in the sintering process.[11] The experimental evidence that oxygen rich α-sialons ($x \fallingdotseq 0{\cdot}3$), which are close to β-sialon in chemical compositions, more easily transform to β-sialons than do nitrogen rich α-sialon[30] supports this assumption. The effect of glassy phase on the transformation of $\alpha \rightarrow \beta$ is also accompanied by the change in chemical composition in sialon grains [as revealed by eqn (1)] and agrees well with this explanation.

Reported results on $\alpha \rightarrow \beta$ phase transformation are mainly examined in $\alpha + \beta$ composites.[14,15] The compositions of α-sialons are thus shifted towards the edge of α-sialon stability range. The stability of α-sialons thus largely depends on the shift of chemical composition in sialon grains. This is why the α/β ratio after annealing depends largely on the starting composition and the kind of stabilizing metal as reported by several papers.[11,14,15]

In the present work, the solubility (x) in starting α-grains is higher than the minimum value of 0·3. Therefore, there was no $\alpha \rightarrow \beta$ transformation in Dy-, Y- and Yb- α-sialon because the x values after annealing still remain in the range $x > 0{\cdot}3$. Thus the effect of temperature on $\alpha \rightarrow \beta$ phase transformation is related to the lower solubility (x) in α-sialon grains or the occurring of chemical reaction of α-sialon with the oxide grain boundary phase at low temperature.

4 Conclusion

The stability of α-sialon in low temperature annealing was examined in an α-sialon + rare eath garnet (RAG) composition using Nd_2O_3, Dy_2O_3, Y_2O_3 or Yb_2O_3 as the stabilizing oxide. In the Dy-, Y- or Yb-system, only crystallization of the RAG phase was observed without phase transformation from α to β. The decrease of solid solubility (x) in the Dy- and Y-systems was also detected after annealing. In contrast, the transformation $\alpha \rightarrow \beta$ was detected in the composite ($\alpha + \beta + M'$) of the Nd-system. The experimental result on the

instability of Nd-α-sialon at low temperature was explained by the shift of solid solubility (x) out of the stability range in terms of solubility change and chemical reaction with the grain boundary phase.

References

1. Mitomo, M. and Tajima, Y., Sintering, properities and applications of silicon nitride and sialon ceramics. *J. Ceram. Soc. Jpn*., 1991, **99**, 1014–1025.
2. Jack, K. H., Sialons and related nitrogen ceramics. *J. Mater. Sci*., 1976, **11**, 1135–1158.
3. Ishizawa, K., Ayuzawa, N., Shiranita, A., Takai, M., Uchida, N. and Mitomo, M. Some properites of α-sialon ceramics. In *Proceeding of Second International Symposium on Ceramic Materials and Components for Engines,* ed W. Bunk and H. Hausner. Deutsche Keramische Gesellschaft, Bad Honnef, Germany, 1986, pp. 511–518.
4. Cao, G. Z. and Metselaar, R., α-Sialon ceramics: a review. *Chem. Mater*., 1991, **3**, 242–252.
5. Ekström, T. and Nygren, M., SiAlON ceramics. *J. Am. Ceram. Soc*., 1992, **75**, 259–276.
6. Huang, Z. K., Tien, T. Y. and Yen, T. S., Subsolidus phase relationships in Si_3N_4-AlN-rare-earth oxide systems.. *J. Am. Ceram. Soc*., 1986, **69**, C–241–C-242.
7. Sun, W. Y., Tien, T. Y. and Yen, T. S., Solubility limits of α-SiAlON solid solutions in the system Si,Al,Y/N,O. *J. Am. Ceram. Soc*., 1991, **74**, 2547–2550.
8. Redington, M., O'Reilly, K. and Hampshire, S., On the relationships between composition and cell dimensions in α-sialons. *J. Mater. Sci. Lett*., 1991, **10**, 1228–1231.
9. Bartek, A., Ekström, T., Herbertsson, H. and Johansson, T., Yttrium α-sialon ceramics by hot isostatic pressing and post-hot isostatic pressing. *J. Am. Ceram. Soc*., 1992, **75**, 432–439.
10. Mandal, H., Thompson, D. P. and Ekström, T., Reversible $\alpha \Longleftrightarrow \beta$ sialon transformation in heat-treated sialon ceramics. *J. Eur. Ceram. Soc*., 1993, **12**, 421–429.
11. Mandal, H., Camuseu, N. and Thompson, D. P., Comparison of the effectiveness of rare-earth sintering additives on the high-temperature stability of α-sialon ceramics. *J.Mater. Sci*., 1995, **30**, 5901–5909.
12. Shen, Z., Ekström, T. and Nygren, M., Temperature stability of samarium-doped α-sialon ceramics. *J. Eur. Ceram. Soc*., 1996, **16**, 43–53.
13. Zhao, R., Cheng, Y.-B. and Drennan, J., Microstructural features of the α to β-sialon phase transformation. *J. Eur. Ceram. Soc*., 1996, **16**, 529–534.
14. Shen, Z., Ekström, T. and Nygren, M., Relations occuring in post heat-treated, α/β-sialons: On the thermal stability of α-sialon. *J. Eur. Ceram. Soc*., 1996, **16**, 873–883.
15. Camuscu, N., Thompson, D. P. and Mandal, H., Effect of starting composition, type of rare earth sintering additive and amount of lquid phase on $\alpha \Longleftrightarrow \beta$ sialon transformation. *J. Eur. Ceram. Soc*., 1997, **17**, 599–613.
16. Zhao, R. and Cheng, Y. B., Decomposition of Sm α-SiAlON phases during postsintering heat treatment. *J. Eur. Ceram. Soc*., 1996, **16**, 1001–1008.
17. Falk, L. K. L., Shen, Z.-J. and Ekström, T., Microstructural stability of duplex α-β-sialon ceramics. *J. Eur. Ceram. Soc*., 1997, **17**, 1099–1112.
18. Ekström, T., Falk, L. K. L. and Shen, Z.-J., Duplex α, β-sialon ceramics stability by dysprosium and samarium. *J. Am. Ceram. Soc*., 1997, **80**(2), 301–312.
19. Shen, Z. and Nygren, M., On the extension of the α-sialon phase area in yttrium and rare-earth doped systems. *J. Eur. Ceram. Soc*., 1997, **17**, 1639–1645.
20. Wang, H., Sun, W.-Y., Zhuang, H.-R. and Yen, T-S., Preparation of R-α′-β′-sialons (R = Sm, Gd, Dy, Y and Yb) by pressureless sintering. *J. Eur. Ceram. Soc*., 1994, **13**, 461–465.
21. Min, J.-W. and Mitomo, M., Preparation of Y-α-sialon with glassy or crystalline phase at grain boundaries. *Ceram. Int*., 1995, **21**, 427–432.
22. Shen, Z., Ekström, T. and Nygren, M., Homogeneity region and thermal stability of neodymium-doped α-sialon ceramics. *J. Am. Ceram. Soc*., 1996, **79**(31), 721–732.
23. Ekström, T., Kaell, P. O., Nygren, M. and Olsson, P. O., Dense single-phase β-sialon ceramics by glass-encapsulated hot isostatic pressing. *J. Mater. Sci*., 1989, **24**, 1853–1861.
24. Shen, Z., Aslikin, D., Babuslikin, O. and Ekström, T., Melilite formation in a samarium-stabilized α-sialon ceramics during postsintering heat treatment. *J. Am. Ceram. Soc*., 1997, **80**(31), 817–821.
25. Menon, M. and Chen, I. W., Reaction densification of α'-sialon II, Densification behavior. *J. Am. Ceram. Soc*, 1995, **78**, 553.
26. Hwang, S. L. and Chen, I. W., Reaction hot pressing of α' and β'-SiAlON ceramics. *J. Am. Ceram. Soc*., 1994, **77**, 165–171.
27. Bandyopadliyay, S., Hoffmann, M. J. and Petzow, G., Densification behaviour and properties of Y_2O_3-containing α-sialon-based composites. *J. Am. Ceram. Soc*., 1996, **79**, 15–37.
28. Nishimura, T., Ishida, A. and Mitomo, M., to be submitted.
29. Jack, K. H., Sialon ceramics: retrospect and prospect. In *Silicon Nitride Ceramics-Scientific and Technological Advances*, ed. I. W. Chen, P. F. Becher, M. Mitomo, G. Petzow and T. S. Yen. Mater. Res. Soc., Pittsburgh, U.S.A., 1993, pp. 15–27.
30. Mandal, H. and Thompson, D. P., Mechanism for $\alpha \Longleftrightarrow \beta$ sialon transformation. *Fourth Euro Ceram.* Vol. 2, ed. C. Galassi. Gruppo Editoriate Faenza, Italy, 1996, pp. 327–334.